J Mater Sci: Mater Med (2009) 20:711–718
DOI 10.1007/s10856-008-3629-5

A novel nano hydroxyapatite-incorporated Ni–P coating as an effective inter layer for biological applications

S. M. A. Shibli · A. C. Jayalekshmi

Received: 1 May 2008 / Accepted: 16 October 2008 / Published online: 6 November 2008

Abstract Hydroxyapatite (HA) coatings are normally made directly on orthopaedic implants and they possess many demerits such as cracks, irregular phase composition and poor adhesion. The present study had a novel approach of providing a nano-HA and phosphorous-rich electroless nickel (EN) coating as an interlayer on stainless steel (SS) prior to electrodeposition of pure HA coating. The interlayer had the merits of having incorporated with nano HA with rich phosphorous content. The outermost HA coating had excellent adherence and it was found to be free from any defects since it was formed only on the interlayer and not on the direct substrate. The overall coating system revealed high bioactivity when immersed in simulated body fluid (SBF). The present study also highlights the scope of using cost effective SS as the implant substrate instead of titanium as against the current trend of substrate selection.

1 Introduction

Hydroxyapatite (HA) is the natural bone mineral ($Ca_{10}(PO_4)_6(OH)_2$, Ca/P ratio 1.67) and hence, it is applied as a coating on the surfaces of implants to improve the fixation between hard tissues and the metal implants [1, 2]. Extensive reports are available on chemical modification of such coatings to improve their adhesion on the substrate. For titanium substrates, a HA/TiO_2 double layer coating can be applied for improved adhesion [3]. Reinforcing materials such as ZrO_2 and SiO_2 can be used for composite coatings with HA [4, 5]. The composite coatings generally have a fairly good chemical stability, erosive endurance and dissolution resistance [6]. Development of cobalt/HA composite coatings with increased adhesion have also been reported [7]. Cobalt alone is not a satisfactory choice for implantation purpose and hence nickel, the next element to cobalt can be used for such composite coatings. The bonding strength of Ni–HA composite coatings are generally much higher than that of pure HA coatings [8]. The methods of electrodeposition [9, 10] and electro-co deposition [11] can be adopted to fabricate such Ni–HA composite coating.

Normally, most of the hydroxyapatite coatings that are directly made on orthopaedic implants possess many demerits such as cracks, irregular phase composition and poor adhesion. The present study had a novel approach of providing a nano-HA and phosphorous-rich electroless nickel (EN) coating as an interlayer on stainless steel (SS) prior to electrodeposition of pure HA coating. This is against the current trend of ignoring cost effective SS as the substrate for implants. The method of electroless nickel plating (EN) can yield the merits such as uniform coating on any surface, easy control of parameters and controlled composite reinforcement. Nano HA was incorporated in the inter layer to provide effective adhesion during the successive formation of pure HA top layer. i.e., The HA–Ni–P coating could serve as an effective pre-coat for the successive development of HA coating. Also the interlayer could prevent the any release of metal ions from the SS substrate. Having these points as the background, the present work was designed with new methodology and the detailed results are discussed in this paper.

S. M. A. Shibli (✉) · A. C. Jayalekshmi
Department of Chemistry, University of Kerala, Thiruvananthapuram, India
e-mail: smashibli@yahoo.com

2 Material and methods

2.1 The substrate and the pre-treatment method

Type 316L SS strips of dimension 3 × 2 × 0.2 cm^3 were used as the substrate. The strips were polished with 120-grit SiC paper and then immersed in a mixed acid solution containing HNO_3 (150 g/l) and HF (50 g/l) for 5 min at room temperature (30 ± 2°C). The strips were then activated by Wood's nickel strike (ASTM B656) prior to electroless coating.

2.2 The electroless nickel plating bath

The electroless plating bath selected for the present work, after preliminary screening and optimization, had the composition, Nickel sulphate heptahydrate: 30 g/l (spectrochem, 99%), sodium hypophosphite: 25 g/l (spectrochem, 99%), and succinic acid: 25 g/l (NICE, 99%) which is similar to a literature report [12]. The hydroxyapatite particles, prepared as described elsewhere [13] was added in different proportion (0–100 g/l) during the process of electroless deposition, with constant stirring. The deposition process was carried out at 80 ± 1°C for 2 h at a pH of 4.5.

2.3 Characterization of the coating

2.3.1 Physico chemical characterization

The prepared HA powder was characterized by XRD (X'pert software) analysis and the particle size was evaluated by TEM analysis (TEM, 2000FX-11, TEM, JEOL, Japan). The thickness of the coating was tested as per a report available in literature [14]. In this method the deposition was carried out on a particular surface area (A) and the weight of the coating before and after the deposition was evaluated. The difference in weight of the coating was noted as Δw. The thickness was evaluated by the equation, $t = (A \times \rho)/\Delta w$ where 't' is the thickness of the coating; 'A' is the coated surface area and 'ρ' is the density of the coating. The surface morphology was analyzed using a scanning electron microscope (SEM, HITACHI S 4000) after cleaning the surface with distilled water, acetone and then drying. The samples were applied with a very thin gold coating using a Polaron SC7620 sputter coater, to prevent surface charging effect and their porosity was analyzed by SEM. The adherence of the HA-incorporated Ni–P coating was tested by brushing with a standard brush and inspected for any micro level exposure of the substrate. The micro level exposure of the substrate was detected by means of noting the development or change in variation of the surface potential of the coated surface when immersed in a stagnant simulated body fluid (SBF) at 37 ± 0.5°C with an impression of anodic current. The surface potential was measured with reference to a saturated Calomel Electrode (SCE). The prepared Ni–P and HA–Ni–P coatings were also characterized by XRD (X' pert software) analysis.

2.3.2 Electrochemical characterization

The trend of open circuit potential (OCP) vs time, was monitored by immersing the coatings (1 cm^2 area), in a stagnant 0.9% NaCl solution (50 ml) at 37 ± 0.5°C [15]. The OCP was measured with reference to SCE. The anodic polarization experiments were carried out using a potentiostat of BAS after immersing the coated specimens in a stagnant 50 ml Ringer's solution [16] at 37 ± 0.5°C. The coated specimens were fixed as the working electrodes, a platinum mesh as the counter electrode while SCE was the reference electrode.

Electrochemical impedance spectroscopic (EIS) studies were carried out using an Autolab PGSTAT 30 plus FRA 2 corrosion measurement system. The equivalent circuit used was R1(C1[R2(R3C2)]) which got fitted very close to the experimentally obtained values. The impedance analysis was carried out using Ringer's physiological solution as the electrolyte. Ag/AgCl, Pt and the specimen having 1 cm^2 exposed area, were used as reference, counter and working electrodes respectively. The impedance analysis was carried out at a frequency range of 1 to 10 Hz, with reference to OCP after 30 min of exposure of the specimens in the electrolyte. In all these experiments duplicate specimens were included to ensure reproducibility.

2.3.3 Bioactivity

The bioactivity of the developed coatings was evaluated using simulated body fluid (SBF), whose ion concentration was similar to that of human blood plasma. The SBF solution was buffered at pH 7.4 using tris(hydroxylaminomethane). The HA–Ni–P coated specimen was soaked in SBF for a period of 14 days at 37 ± 0.5°C without stirring and the resultant pH was monitored. Optical micrographs (Olympus SZ 61) of the coatings were recorded to evaluate the extent of the HA growth. The SBF solution after the deposition was tested for any probable release of Ni^{2+} ions from the coating, using dimethyl glyoxime reagent.

2.4 HA coating on HA–Ni–P inter layer

The HA-incorporated Ni–P coating was further made biocompatible by forming a pure HA top layer by electrodeposition followed by an alkaline treatment [17, 18]. The developed HA coatings were subjected to heat treatment at 800°C to make the coating adherent to the substrate. Preliminary evaluation of the CaP coating was

carried out in order to assess its adherence to the substrate, by scratching with a sharp blade followed by repeated washing in distilled water. The surface morphology and the cross sectional view of the HA coating on the HA–Ni–P interlayer were evaluated by SEM analysis. The samples were applied with a very thin gold coating, using Polaron SC7620 sputter coater, to prevent surface charging effect.

The extent of additional bio growth of HA over this top HA coating was studied after soaking the coating in SBF. The surface morphology of the biomimetically developed coating was evaluated by using an optical microscope (Olympus SZ 61, Taiwan). The composition of the HA coating was evaluated by EDS analysis. The energy dispersive X-ray analysis (EDS) of the coating was carried out using an EDAX instrument of Oxford make. In all these experiments duplicated specimens were included to ensure reproducibility.

3 Results

3.1 Modification of electroless nickel coating by HA incorporation

The hydroxyapatite (HA) particles prepared during the present work were found to be of nanometer in size. The nano size of the HA powder was confirmed by XRD and TEM analyses (Figs. 1 and 2). The HA powder showed 2θ values of 25.88° for reflection at (202), 31.78°, 32.19° and 32.90° for reflections at (211), (112), (300) and 34.07° at (002). The peaks were comparable to that of the pure HA powder. XRD analysis revealed that the crystalline size of the prepared HA particles were 0.97 nm. The crystalline size was determined by the Scherrer formula, $D = 0.9\ \lambda/\beta \cos\theta$. The particle size of the HA powder was found to be below 50 nm during TEM analysis.

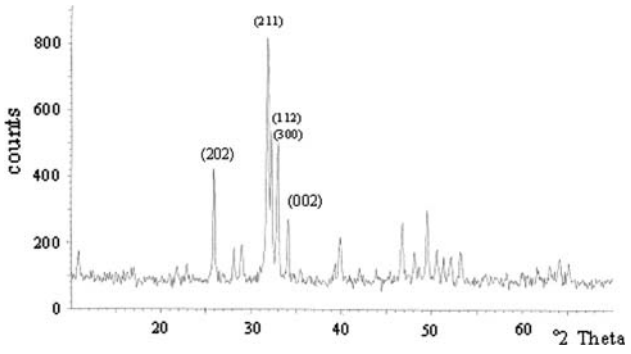

Fig. 1 The XRD image of the prepared HA powder

The hydroxyapatite particles were incorporated into the coating by means of adding them into the electroless bath during the deposition process. The HA incorporated Ni–P coating was found to be less porous than the pure Ni–P coating. The thickness was evaluated by the equation $t = (A \times \rho)/\Delta w$, where t is the thickness of the coating; A is the coated surface area, ρ is the density of the coating and Δw is the weight difference of the coating before and after the deposition process. The coating had uniform thickness (5 μm) all over the substrate exposed into the bath. The adherence of the HA incorporated Ni–P coating was tested by brushing with a standard brush resulting in micro level exposure of the substrate in few cases. The micro level exposure of the substrate could be detected by means of noting the development or change in variation of the surface potential of the coated surface when immersed in a stagnant simulated body fluid (SBF) at 37 ± 0.5°C and by applying an anodic current. The variation in surface potential of the coating observed after such scratch test followed by immersion in SBF is given in Fig. 3. The coating after the scratch test exhibited a stable potential up to 1.3 mA/cm^2. This revealed that the coating could be stable in SBF even if some destruction takes place. Microscopic and visual destruction were also made to support this inference.

3.2 Compositional analysis

The XRD pattern of the pure Ni–P coating and the HA-incorporated Ni–P coating are shown in Fig. 4. The peaks

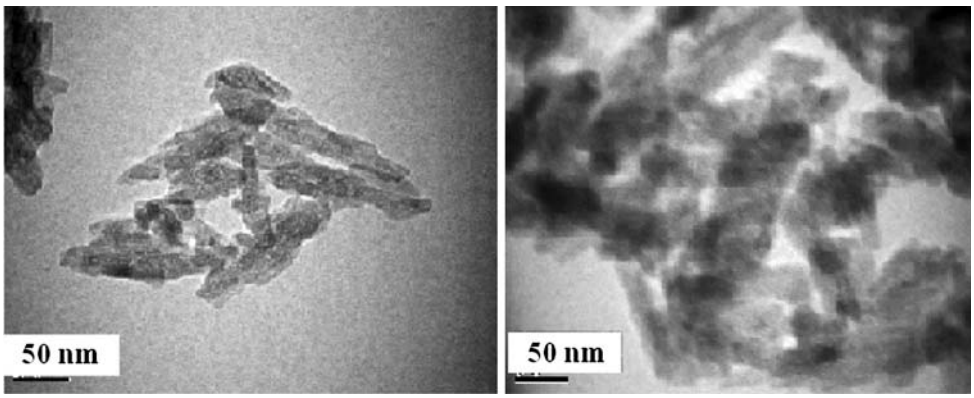

Fig. 2 The TEM image of the prepared HA powder

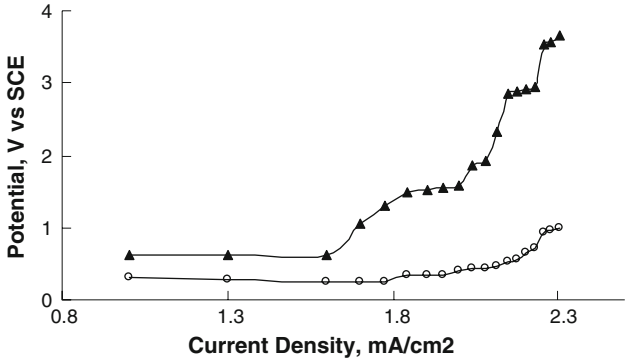

Fig. 3 The variation of potential during anodic polarization of the coating after scratch test followed by dissolution in simulated body fluid (○—coating before scratch, ▲—coating after scratch test)

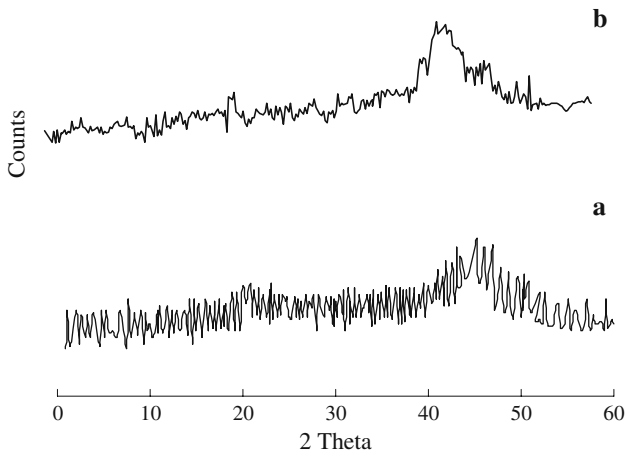

Fig. 4 The XRD patterns of the (a) Ni–P coating and (b) HA–Ni–P layer

corresponding to Ni (111) and Ni (200) were depicted in the NiP and the HA–Ni–P coatings. Figure 4b reveals the microcrystalline nature of the coating. No peaks corresponding to HA were found in the XRD pattern. The phosphorous content in the EN coating generally varied between 3–14% depending on the deposition conditions and the bath used [19, 20]. In the present case the phosphorous content increased due to the incorporation of HA into the coating. A detailed evaluation on the role of phosphorous was not under the purview of the present work.

3.3 Morphological analysis

The surface morphology of the coating exhibited in Fig. 5 revealed the non-porous nature of the coating. A uniform coating of Ni–P layer was found in the micrographs of pure and the HA-incorporated Ni–P coatings. The HA-incorporated Ni–P coating had a thicker growth and its appearance differed from that of the pure Ni–P coating. The HA particles were visible all over the substrate. They got embedded into the Ni–P matrix. The nano size HA particles were got incorporated into the Ni–P matrix of 5 μm thickness. The surface morphology of the electrodeposited HA coating (Fig. 6a) exhibited uniform needles like crystals of HA on the surface. The surface morphology of the cross sectional image of the electrodeposited coating (Fig. 6b) exhibited a dense HA layer above the HA–NiP layer.

3.4 Influence of the amount of HA

The effect of the amount of HA present in the modified coating on the prevention of corrosion of the stainless steel substrate was analyzed electrochemically. The corrosion resistance was evaluated based on the trend of variation of the open circuit potential (O·C.P) with time, i.e. the equilibrium potential of the anode (the coated specimen) when it was in contact with the electrolyte. It signifies the tendency of the metal to corrode and change its potential with time without the application of an external current. This potential variation can be related to important phenomena occurring at the metal surface. The OCP values were found to be more anodic (Fig. 7) as a function of increase in the amount of HA in the coatings. The coating incorporated with 100 g/l of HA exhibited the maximum noble OCP values i.e., OCP decay was very low in that case. The

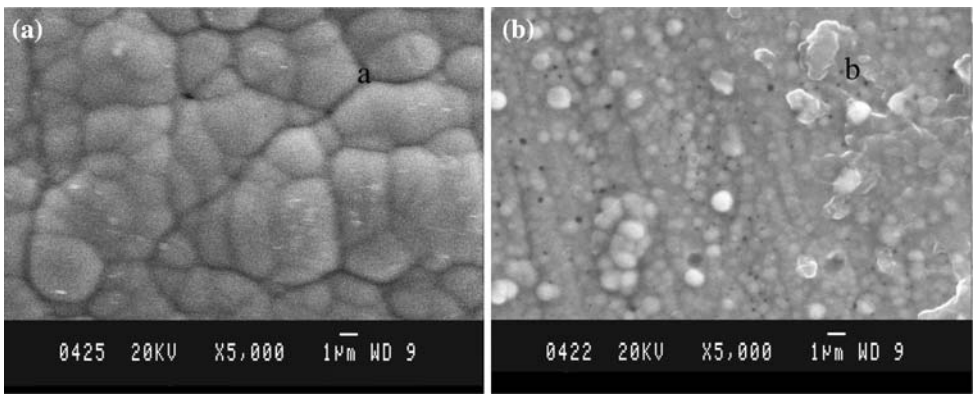

Fig. 5 The scanning electron micrographs **a** Ni–P coating and **b** HA–Ni–P coating

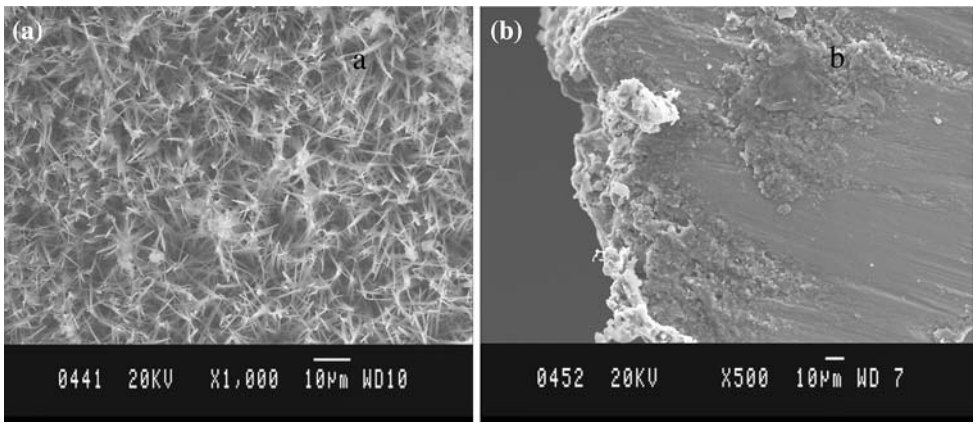

Fig. 6 The scanning electron micrographs **a** HA coating electrodeposited on the HA–Ni–P coating and **b** Cross sectional image of (**a**)

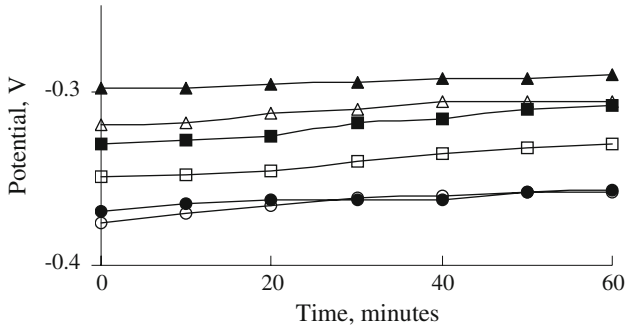

Fig. 7 The variation of the open circuit potential of the Ni–P coating with varying amount of HA (●: 0 g/l; ○: 0.01 g/l; □: 0.1 g/l; ■: 1 g/l; Δ: 10 g/l; ▲: 100 g/l)

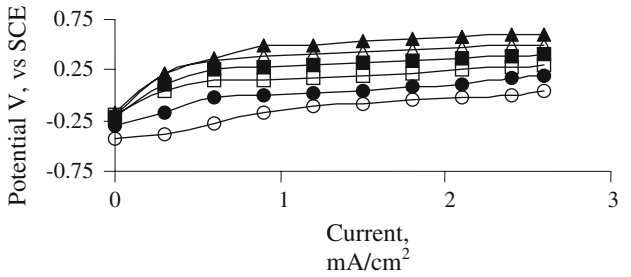

Fig. 8 The anodic polarization curves of NiP coating with varying amount of HA (●: 0 g/l; ○: 0.01 g/l; □: 0.1 g/l; ■: 1 g/l; Δ: 10 g/l ▲: 100 g/l)

anodic polarization curves of the HA-incorporated Ni–P coating is given in Fig. 8. The increase in the HA content of the coating resulted with maximum polarization revealing high corrosion resistance of the coating. Based on the polarization experiments also, it was inferred that the amount of 100 g/l HA yielded the best characteristics to the coating to protect the SS substrate from undergoing any corrosion. The increase in the HA content caused appreciable changes in the potential value for small variations in the current impressed, revealing the improved corrosion resistance nature of the HA-rich Ni–P layer.

The Niquiste plot showing the corrosion resistance nature of the coating is exhibited in Fig. 9. The HA–NiP layer (Fig. 9b) exhibited a semicircle having lesser area compared to the Ni–P coating. The R1, R2, R3 values of Ni–P and HA–Ni–P coatings were 19.53 ± 3.078 Ω, 1.380 ± 14.32 kΩ, −1000.0 ± 100.000 GΩ and 10.77 ± 3.672 Ω, 122.3 ± 25.268 Ω, 1.503 ± 10.796 kΩ, respectively. The C1 and C2 values of Ni–P and HA–Ni–P coatings were 203.8 ± 4.804 μF, 0.504 ± 16.762 mF and 204.2 ± 8.507 μF, 254.8 ± 12.809 μF, respectively. The Chi-square values were found to be 1.8013E + 00 and 2.3403E + 00. The HA incorporated coating exhibited high corrosion resistance.

3.5 Biocompatibility of the coating

An effective growth of the HA after immersion in SBF for 2 weeks, was clearly revealed in the optical micrographs (Fig. 10). The optical micrographs revealed uniform growth of HA particles. The presence of HA particles served as nucleation sites for further growth of HA. The top layer was found to be uniform. There was a release of trace of Ni^{2+} ions during the initial days, but the nickel ion release was stopped after the uniform growth of HA layer. There was no Ni^{2+} ion present in the SBF after a prolonged immersion of the coated specimen. The pH of the coating increased slightly from 7.4 to 7.8 for the initial period of the immersion study and then decreased to 7.5 at the end. The Ca/P ratios as analyzed by EDS revealed that the coating obtained by biomimetic deposition was HA having the Ca/P ratio 1.67.

3.6 Prevention of the release of Ni^{2+} ions

Pure HA coating was developed on the HA-incorporated Ni–P coating in order to prevent any probable Ni^{2+} ion release from the inner coating. The pure HA outer coating was developed by electrodeposition followed by an alkaline treatment as discussed in Sect. 2.4. The outer layer of

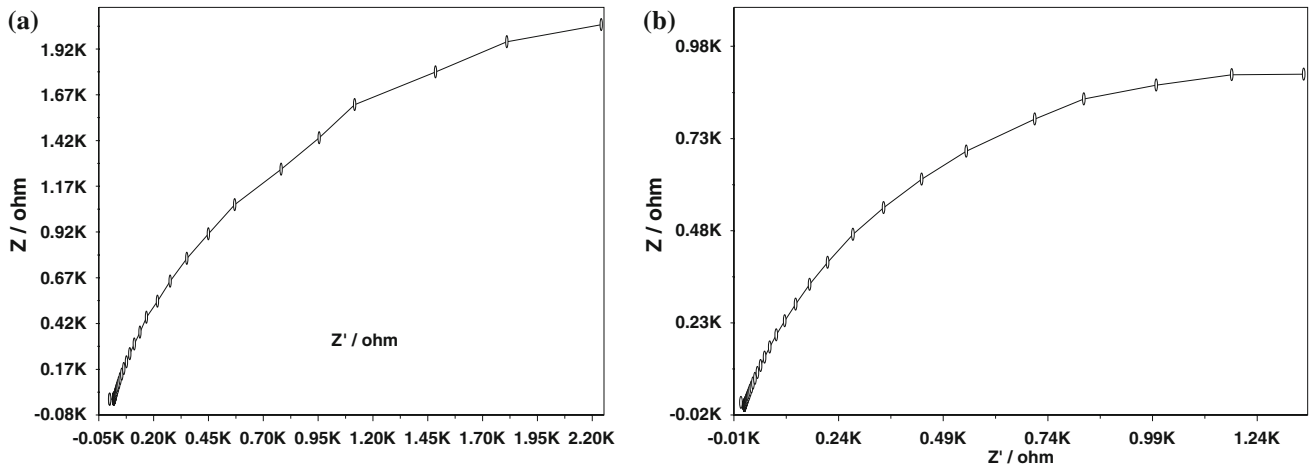

Fig. 9 The Niquiste plot showing the corrosion resistance behaviour of **a** Ni–P coating and **b** HA–Ni–P coating

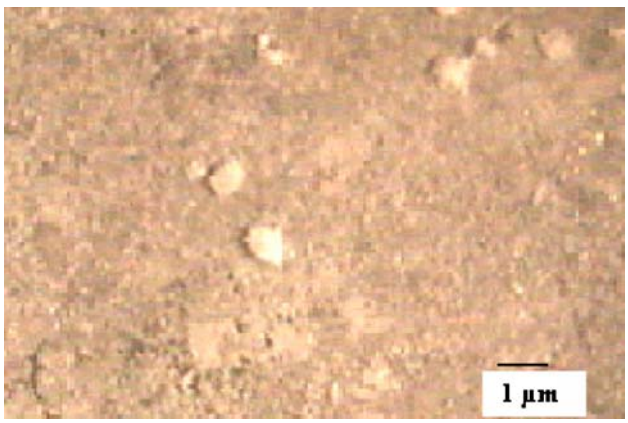

Fig. 10 HA incorporated Ni–P coating after immersion in SBF for 14 days

the coating was found to be uniform and pore free throughout the surface as evidenced in the scanning electron micrographs (Fig. 6a). The adhesion of the coating was also found to be good. The middle HA-incorporated Ni–P layer between the substrate and the pure HA outer layer of the coating acted as a binding layer for the outermost HA layer on the substrate. There was no Ni^{2+} ion release from the overall coating system when the coated specimen was immersed in SBF.

4 Discussion

4.1 Role of HA in the Ni–P coating

The incorporation of HA into pure EN coating minimized the porosity and improved the adhesion of the Ni–P layer on the SS substrate. The HA particles acted as the nucleation sites during development of the coating. There was uniform distribution of the HA particles throughout the three dimensional matrix of the coating. The surface morphology was found to be competent to other early report of HA–Ni composite coatings [11]. The HA particles got dispersed in the Ni–P layer during the electroless deposition process. From the literature it is evidenced that adsorption of Ni^{2+} by HA is proceeded by means of cationic/anionic grouping [21]. During the electroless deposition process the HA particles would get adsorbed with nickel ions and both get a positive charge and move towards the SS substrate. On the substrate the HA incorporated nickel ions would get reduced. The vigorous stirring of the electroless bath would also facilitate the adsorption. The reduced layer formed over the substrate could act as nucleation site for further Ni^{2+} reduction and a uniform Ni–P layer is formed all over the SS substrate. The HA particles would get trapped inside the Ni–P matrix. As the HA particles have nano size they could better be incorporated into the HA matrix. The incorporated HA had crystalline nature. i.e., during deposition no chemical change took place with the added powder and it just got trapped in the Ni–P matrix.

The electrochemical impedance of the coating revealed that the HA–Ni–P coating had higher corrosion resistance compared to Ni–P coating. The R1, R2 and R3 values of HA incorporated coating was found to be lower than that of Ni–P coating. This revealed the role of HA in the prevention of intrusion of Cl^- ions into the Ni–P layer.

4.2 Influence of the amount of HA content

From the trend of the variation of OCP of the coatings with time (Fig. 7) it was clear that the increase in the amount of HA caused a potential shift to more anodic region. The maximum amount of HA-incorporated coating showed the maximum corrosion resistance. The polarization data also revealed that the variation of potential with respect to the

applied current was low for the coatings having higher amount of HA. The presence of larger amount of HA content caused maximum corrosive resistance. Generally the extent of phosphorous content determines the structure, corrosion resistance and hardness of the alloy-coating layer. The HA enrichment resulted in the added advantage of the increase in the phosphorous content and suppressed the corrosion of the inner substrate to a little extent. Increasing the HA concentration above 40 g/l may bring the hardness and thickness values independent of the concentration [22]. As per the literature 90 g/l is the optimum amount of HA in the electrodeposited nickel coating [9]. In the present study 100 g/l HA incorporated coating performed better and it was chosen as the optimum amount of HA. Increasing the amount of HA content beyond a certain limit might decrease the adhesion of the coating to the SS.

4.3 Biocompatibility of the HA incorporated Ni–P layer

Effective HA growth was observed on the surface of the coating when immersed in SBF. On immersing the coating in SBF the HA particles in the HA incorporated Ni–P coating got exposed initially due to the release of Ni^{2+} ions from the coating into the SBF solution. The incorporated HA particles came into contact with the Ca^{2+} ions present in the SBF and formed the nucleation sites for further HA growth. The presence of nickel ions in the SBF solution revealed this process. Due to the prolonged growth of HA, the release of Ni^{2+} ion was suppressed and hence a uniform HA coating was obtained as shown in Fig. 10. The variation of pH of the SBF solution may be due to the deposition of Ca^{2+} and PO_4^{3-} ions into the coating and due to the release of nickel ions. But at the end of the study period the pH decreased i.e., the release of Ni $^{2+}$ was suppressed. The ratio of Ca/P (1.67) revealed that the coating obtained was pure HA.

4.4 Role of HA-incorporated Ni–P layer on the formation of HA top layer

Chromium or nickel ions if released in body can cause allergy and they are also carcinogens. In the present case, the prevention of any probable release of Ni^{2+} ions through the coating system could be achieved by providing a uniform pure HA coating over the HA–Ni–P layer. This was achieved by means of electro deposition. During cathodic deposition, $Ca^{2+}$and PO_4^{3-} ions may get precipitated from the solution and the deposited coatings could be converted into HA coating [17, 18]. The alkaline treatment could convert the calcium phosphate into hydroxyapatite. Thus a pure and adherent HA coating could be formed on the substrate. This was achieved in the present case and the present coating system was not only free from any probable release of harmful ions but also had the characteristics of facilitating normal growth of HA when kept in body environment.

4.5 The mechanical strength and the biocompatibility of the coating

In the present study an EN plate with high phosphorous content was achieved due to the incorporation of HA. The phosphorous content of the coating could control the release of nickel ion and hence the corrosion of coating system. In the present case the effect of thermal expansion-mismatch between the metallic substrate and the hydroxyapatite coating was minimized by means of providing a Ni–P interlayer. The coefficient of thermal expansion of Ni, SS and HA become close at high temperature around 1000°C [23]. The superficial HA coating was found to be to a large extent adherent to the substrate. Sintering at 800°C made the HA coating more adherent. In the present case there were no micro cracks in the outward HA coating, even at 800°C, as it was formed on the HA–Ni–P interlayer and not on the pure SS substrate. It was evidenced during microscopic analysis also.

5 Conclusion

The present methodology and the process of surface engineering demonstrated in the present work for providing a phosphorous-rich Ni–P–HA interlayer were found to be highly effective. The HA-incorporated Ni–P interlayer had high biocompatibility in terms of forming uniform pure HA layer when immersed in SBF. The outermost pure HA layer effectively suppressed any probable release of Ni^{2+} ion through the interlayer. The outermost HA coating had excellent adherence and it was found to be free from any defects as it was formed only on the interlayer and not on the substrate. The overall coating system had high biocompatibility revealing the tendency of facilitating effective further growth if actually implanted in body. The rich in phosphorous content of the layer were one of the merits of the present coating system. The present results advocate that still there is a significant scope for SS to be considered as the substrate for implants though the present trend is against the same. Secondly, the methodology of compositional based layer-wise structural modification would be significantly better than a single layer-based system as extensively reported currently. Thirdly, utilization of nano HA would be more advantageous than micro HA during surface engineering.

Acknowledgements The authors are grateful to the Prof. & Head, Dept. of Chemistry, University of Kerala for his kind encouragement and for extending facilities to complete this work. They are also grateful to Kerala State Council for Science, Technology and Environment (KSCSTE), Govt. of Kerala for providing financial assistance.

References

1. S. Robler, A. Sewing, R. Born, D. Scharnweber, M. Dard, H. Worch, J. Biomed. Mater. Res: A **64**(A), 655 (2003)
2. L.L. Sun, C.C. Berndt, K.A. Gross, A. Kucuk, J. Biomed. Mater. Res. Appl. Biomater. **58**, 570 (2001). doi:10.1002/jbm.1056
3. C.M. Lin, S.K. Yen, Biomaterials **21**, 841 (2005)
4. A. RapaczKmita, A. Stosarczyk, Z. Paszkiewicz, Ceram. Int. **31**, 567 (2005). doi:10.1016/j.ceramint.2004.06.022
5. A. Saenz, M.L. Montero, V.M. Castano, Surf. Rev. Lett. **9**, 1799 (2002)
6. X. Xiu-Feng, L. Rong-Fang, Z. You-Song, L. Lan-Yun, X. Dao-Xuan, Yingyong Huaxue **21**, 687 (2004)
7. H. Dasarathy, C. Riley, H.D. Coble, W.R. Lacefield, G. Maybee, J. Biomed. Mater. Res. **31**, 81 (1996). doi:10.1002/(SICI)1097-4636(199605)31:1<81::AID-JBM10>3.0.CO;2-P
8. L. Rongfang, X. Xiufeng, Z. Yousong, Cailiao Baohu **36**, 28 (2003)
9. B. Xiaojun, L. Hairong, C. Zongzhang, Cailiao Baohu **32**, 5 (1999)
10. I. Hairong, C. Zongzhang, B. Xiaojun, Wuji Cailiao Xuebao **13**, 913 (1998)
11. H. Liping, L. Hairong, C. Dachuan, C. Zongzhang, B. Xiaojun, Surf. Coat. Tech. **160**, 109 (2002). doi:10.1016/S0257-8972(02)00413-9
12. G. Lu, G. Zangari, Electrochim. Acta **47**, 2969 (2002). doi:10.1016/S0013-4686(02)00198-6
13. A. Osaka, Y. Miura, K. Takeuchi, M. Asada, K. Takahashi, J. Mater. Sci.: Mater. Med. **2**, 51 (1991). doi:10.1007/BF00701687
14. I. Paseka, Electrochim. Acta **40**, 1633 (1995). doi:10.1016/0013-4686(95)00077-R
15. S. Kannan, A. Balamurugan, S. Rajeswari, Electrochim. Acta **50**, 2065 (2005). doi:10.1016/j.electacta.2004.09.015
16. T.M. Sridhar, T.K. Arumugam, S. Rajeswari, M. Subbaiyan, J. Mater. Sci. Lett. **16**, 1964 (1997). doi:10.1023/A:1018511406374
17. J.M. Zhang, C.J. Lin, Z.D. Fen, Z.W. Tian, J. Mater. Lett. **17**, 1077 (1998). doi:10.1023/A:1006619729924
18. G.J. Levinskas, W.F. Neuman, J. Phys. Chem. **59**, 164 (1955). doi:10.1021/j150524a017
19. K.G. Keong, W. Sha, S. Malinov, J. Mater. Sci. **37**, 4445 (2002). doi:10.1023/A:1020641611389
20. K.G. Keong, W. Sha, S. Malinov, J. Alloys Comp. **334**, 192 (2002)
21. M.H. Rachidi, K. Bahja, A. Zrinch, M. Hamad, S. Zaydoun, M. Ferhat, J. Chim. Phys. **96**, 706 (1999). doi:10.1051/jcp:1999166
22. B. Xiaojun, J. Zhangpong, Z. Qiang, L. Jiaoshen, Diandu Yu Huanbao **20**, 6 (2000)
23. A.J. Ruys, M. Wei, A. Branwood, B.K. Milthorpe, C.C. Sorrel, J. Australas Ceram. Soc. **30**, 129 (1994)